1	Development of a Waste-Derived Lignin-Porphyrin Bio-Polymer with Enhanced
2	Photoluminescence at High Water Fraction with Wide pH Range and Heavy
3	Metal Sensitivity Investigations
4	
5	Ho-Yin TSE ^{a+} , Shun-Cheung Cheng ^{b+} , Chi Shun Yeung ^{a*} , Chun-Yin Lau ^a , Wing-Hei Wong ^a ,
6	Chengyu Dong ^a , and Shao-Yuan Leu ^{a*}
7	
8	^a Department of Civil & Environmental Engineering, The Hong Kong Polytechnic University,
9	Hong Kong
10	^b Department of Chemistry, City University of Hong Kong, Kowloon Tong, Hong Kong
11	*Corresponding author: csyeung@polyu.edu.hk ; syleu@polyu.edu.hk , Tel: +852-3400-8322
12	⁺ These authors contributed equally to this work.
13	
14	
15	
16	
17	
18	
19	
20	
21	
22	
23	

Abstract

24

25

26

27

28

29

30

31

32

33

34

35

36

37

38

39

40

41

Lignin is a common by-product of pulping industries. Its diverse functional groups in the polymeric matrix make lignin a superior alternative for carbon-based materials. Porphyrin family is well known in the optical sensing; however, the aggregation caused quenching (AQC) due to the stronger π - π interaction during high poor solvent fraction environment will limit the photoluminescence intensity of porphyrin. In this study, a new lignin-porphyrin (AL-CTPP) polymer was developed, which combines and promotes the functionalities of the two chemicals. In photoluminescence investigation, it demonstrated the emission intensity of AL-CTPP in 600 to 780 nm region was 30-fold stronger than porphyrin alone, when the water-solvent ratio > 90%. Lignin could serve as a stable backbone immobilizing porphyrin, and thereafter prevent the unwanted aggregation of porphyrin and the related aggregationcaused quenching at high water fraction solution with various pH. Furthermore, linear correlations were established between absorption properties of AL-CTPP with concentration of five metal ions (i.e., Mn²⁺, Ni²⁺, Co²⁺, Cu²⁺, and Zn²⁺). With these unique features and long emission wavelength, AL-CTPP showed its enhanced performances for potential bioimaging and environmental applications. Lignin-porphyrin polymer may represent a significant outlet of biorefinery and effective utilization of lignin to fabricate a new functional material could offer significant benefits to support wastes valorization.

42

- Keywords: lignin, porphyrin, photoluminescence, aggregation caused quenching, heavy
- 44 metal sensing

Introduction

Increasing demand of green polymers has triggered intensive research efforts towards sustainable techniques to withdraw and utilize the key building-block chemicals from the lignocellulosic biomass. The existing biorefinery techniques have shown to be effective utilizing carbohydrate based components (i.e., cellulose and hemicelluloses). Lignin, the only renewable and the second most abundant aromatic derived from plant, however, has not yet been widely applied for chemical engineering industries or biorefinery. Lignin is a highly cross-linked macromolecule largely found in the cell walls of vascular plants. It composes of 15-35 percent of lignocellulosic biomass depending on different plant species.² More than 50 million tons of lignin is generated yearly as by-products of pulping industry and most of them have been applied for energy recovery through direct combustion.³ Lignin has many valuable properties rather than low value fuel, such as its high resistance to chemical, thermal, and biological degradation. Lignin showed superior functionality on UV absorbance, antioxidation, and amphiphilicity.⁴ In recent years, lignin and its modified derivatives have been applied in adhesives, components for green composites, etc.⁵⁻⁷. It has been also considered in drugs delivery and bioimaging due to its low cytotoxicity 8 and pH/solvent controllable characteristics. 9, 10 With its biocompatible and environmentally-friendly nature, lignin-based nanoparticles have showed its potential as functional group carriers. 11-13

Porphyrin is a significant functional module found in the nature, such as chlorophyll, heme structures and P450 enzymes. Development of modern porphyrins derivatives have been mostly inspired by its multi-functions and condition-specific applications.¹⁴ The well-known applications of porphyrins is as a fluorescence contrast agent for tumor detection ¹⁵⁻¹⁷ and image-guided surgery.¹⁸ To achieve this function, porphyrin has been selected due to an important advantage on strong absorption band at ~400 nm and intense emission in red/NIR region.^{19, 20} However, porphyrins tend to form π – π stacking aggregates especially in high antisolvent fraction environment. These non-covalent intermolecular forces cause the risk of losing photoluminescence function of porphyrin which was called aggregation-caused

quenching (ACQ).^{21, 22} ACQ limits the maximal fluorescence imaging ability and therefore need to be avoided through physical and/or chemical modifications. For physical methods, matrices are used to cap porphyrins, but the loading content should be carefully controlled in order to avoid porphyrin-porphyrin interactions.²³⁻²⁶ For chemical methods, porphyrins has been linked on polymers to prevent ACQ.^{16, 27-30} Another approach is by adding bulky groups like dextrins ³¹, sugars ³² and polyhedral oligomeric silsesquioxanes (POSS) ³³ onto porphyrins, which result in steric effects and further retain its photoluminescence function.

Lignin is bulky and stable in water; the steric hindrance can hence be introduced to porphyrin molecules for preventing aggregation and the related ACQ in aqueous environment. To the best of our knowledge, applying lignin-based backbone to hinder ACQ of porphyrin in high aqueous media has never been synthesized or tested anywhere. In this paper, alkali lignin was selected for its high abundance and used to synthesize the lignin-based nanoparticles with chemically bonded porphyrin moieties. The proposed structure is shown in figure. 1. The physiochemical properties in different water fractions and pH values were studied and compared with porphyrin monomer as reference. Meanwhile, the metal ion sensing ability of the new functional products was investigated to demonstrate the feasibility of the modified lignin in the real case usages. The combination of the two naturally found structure should lead into new orientation of lignin valorization and stabilization of porphyrin-like structure.

Results and discussion

Alkali lignin (AL) has phenolic and aliphatic hydroxyl groups that can be modified to different chromophores by appropriate reagents. The hydroxyl groups in AL determined by ³¹P NMR analysis was provided in figure. S1. The results showed that there were about 0.35 mmol/g of aliphatic OH groups and 2.57 mmol/g phenolic OH groups present in the lignin. These hydroxyl groups can be functionalized by Mitsunobu reaction, which is a mild and efficient coupling reaction method to convert hydroxyl group to ester.^{34, 35} 5-(4-carboxyl phenyl)-10,15,20-triphenyl porphyrin (CTPP) with one phenylcarboxylic group has been coupled with AL to form AL-CTPP and we intentionally retain another three phenyl groups unsubstituted for future modification. After the one step reaction, dialysis treatment has been used to remove unreacted reagents and small molecules. The proposed structure is shown in figure 1.

For quantifying the degree of functionalization (DF) in AL-CTPP, elemental analysis was performed to detect the nitrogen content in the sample. 36,37 The results are listed in Table 1. Since we have already determined the number of hydroxyl group per gram in the AL, we can calculate the DF by eq 1, where N% is the mole content of nitrogen in the lignin-based polymers; n_{OH} is the mole content of total hydroxyl group in AL, which is 2.92 mmol/g and N_{nitrogen} is the molar ratio of nitrogen in CTPP.

$$N\% = n_{OH} \times 14.00 \times N_{nitrogen} \times DF \tag{1}$$

[Potential location of Table 1]

For the in-depth characterization of AL-CTPP polymer, the ¹H NMR spectra of AL, CTPP and AL-CTPP have been presented in figure 2. Compared with AL, we can clear observe the additional signals in the aromatic protons regions. Two distinct multiplets in 7.8 to 8.3 ppm

and two doublets in 8.31 to 8.45 ppm were observed and they are assigned to the protons of the phenyl ring in CTPP. In the AL-CTPP spectrum, the chemical shift of CTPP protons are move to up-field. This mainly due to the phenyl moieties in lignin polymer exerting shielding effect to surrounding chromophores. Furthermore, UV-vis absorption spectra of AL, CTPP and AL-CTPP in ethanol has been shown in figure 3. Compared with AL and CTPP, the absorption peaks in AL-CTPP did not change much and the characteristic Soret band and Q band from CTPP and absorption band from lignin at 240 to 270 nm were still observed. This showed that the ground state properties of porphyrin moieties are not alerted much. The molecular weight of the CTPP polymer has been measured by gel permeation chromatography (GPC) and the measured M.W. is about 10284 Da.

- 130 [Potential location of Fig. 1]
- 131 [Potential location of Fig. 2]
- 132 [Potential location of Fig. 3]

The nanoparticle of AL-CTPP was prepared using self-assembly treatment and the aggregation and formation of nanoparticles was overserved by SEM images. SEM micrographs of AL-CTPP (figure. 4) clearly showed that they have spherical morphology and very unlike the flaky irregular pieces in porphyrin monomer. Dynamic light scattering (DLS) experiments were performed on the nanoparticle samples and the results showed that AL-CTPP have an average particle size of 90 nm in $f_w = 40\%$, pH = 7 and the size becomes smaller with the addition of water in the solution. The size reduced to 20 nm in $f_w = 80\%$. Various pH values ranging from 3 to 7 were explored for the AL-CTPP nanoparticles by DLS analysis. They show very stable particle size diameter and consistent with previous lignin nanoparticles studies along the pH range. The hydrophobic and π -stacking forces lignin to self-assemble to form nanoparticles in the presence of anti-solvent. These interactions become stronger in high f_w solvent and therefore the particles size of the nanoparticles

becomes smaller. There is an exception in pH 3 solution and this is mainly due to the aggregation of nanoparticles.

[Potential location of Fig. 4]

Optical properties investigation of AL-CTPP nanoparticles in various water content of

different pH

It is well known that porphyrin molecules will tend to aggregate to form nanoparticles in the presence of antisolvent, especially in high water environment. The hydrophobic and π -stacking interaction between porphyrin molecules bring them together to form aggregates in the presence of water. The aggregation morphology can be generally fall into two types, H-and J-aggregation.³⁸⁻⁴² The transition moment in the aggregate will create nonradiative pathway upon excitation.^{40, 43-45} This ACQ effect diminish the emission quantum yield in which limits their fluorescence imaging ability. Here, we immobilized CTPP on lignin polymer matrix to limit their degree of freedom and hence reducing the aggregation in high water environment.

The following discussions which have not been specified is referred to pH 7. In the UV-vis and PL spectra of AL-CTPP in ethanol were shown in figure 3 and the porphyrin monomer CTPP was used as a reference to demonstrate the aggregation effect in high water environment. AL-CTPP retained its typical intense Soret band at 414 nm (ϵ = 1.86 x 10⁵ M⁻¹cm⁻¹) and two Q bands at 512 and 546 nm (figure 3A). Upon light excitation at 425 nm, AL-CTPP has two emission peaks at 652 and 716 nm (figure 3B). For the monomer, CTPP in ethanol showed the same Soret band and Q bands in the visible region. It also had the same emission peaks at 652 and 716 nm in PL spectra. These parallel photophysical properties between AL-CTPP and CTPP indicated that the chemical linkage with lignin polymer does not affect the ground state and excited state of the porphyrin moieties.

To study the aggregation effect in the presence of water, UV-vis absorption and PL spectra of the reference porphyrin monomer CTPP in ethanol/water mixture was shown in figure 5. With increasing f_w , the Soret band absorbance of CTPP was broadened and two different spectral changes were observed, and a redshifted band at 421 nm raised accordingly. Furthermore, at $f_{\rm w} \ge 90\%$, a new blue-shifted broad band raised at 400 nm. These two absorption bands also showed significant decreases in extinction coefficient (figure 5A). This is a typical sign for aggregation formation of porphyrins. 46, 47 At higher f_w , the solubility of hydrophobic CTPP is lower and π stacking and hydrophobic interactions drive the molecules to severely stack together leading to increased aggregation. The dipole-dipole interactions between stacked porphyrins changed the absorption wavelength compared with monomer Soret band absorption.^{38, 39, 48, 49} Meanwhile, the emission intensity of CTPP decreases with the increasing of f_w (figure 5D). The emission intensity at 652 nm is dramatically reduced in $f_{\rm w} \ge 90\%$, which indicates that CTPP is a typical ACQ dye. On the contrary, AL-CTPP demonstrate the reduction of ACQ effect in water dominant conditions. Figure 5B and 5D reveals the changes of UV-vis absorption and PL spectra of AL-CTPP in ethanol/water mixture with different f_w values. Upon increasing f_w , AL-CTPP only shows red-shifted and broadened peaks with decreased extinction coefficient (figure 5B). There was no blue-shifted peak appeared at $f_w \ge 90\%$. Upon gradual addition of water, the emission of AL-CTPP was quenched, because of increased solvent polarity. Further increasing f_w to 70%, the emission quenching becomes stable. This is largely due to the steric hindrance of the decorated lignin polymer and phenyl groups which can isolate the porphyrin chromophores from π – π stacking to aggregated state. With addition of water (poor solvent), lignin polymer shrinks gradually, which limits the freedom of porphyrin groups from stacking and results in a lower aggregation efficiency at higher water contents. As a result, at $f_w \ge 90\%$, the emission intensity of AL-CTPP in 600 to 780 nm is 30-fold stronger than CTPP. This evidence showed that immobilization of CTPP on lignin polymer can greatly enhanced the emission intensity. The pH effect on the emission property of AL-CTPP has been also investigated. For alkaline environment, both AL-CTPP and CTPP perform similar emission property, this is because both chemicals are soluble in alkaline solution. However, in acidic environment, the emission

173

174

175

176

177

178

179

180

181

182

183

184

185

186

187

188

189

190

191

192

193

194

195

196

197

198

199

200

intensity of CTPP decrease more significantly. CTPP starts to aggregate in acidic environment and ACQ effect becomes dominant. The PL spectra of AL-CTPP and CTPP in pH from 3 to 7 & $f_{\rm w} \geq$ 90% is shown and compared in figure 5C. The emission intensity of AL-CTPP is dramatically stronger than CTPP 10 to 30 folds in this condition. The large emission enhancement of AL-CTPP indicates that it is a good candidate for bioimaging application in various pH range.

208

202

203

204

205

206

207

209

210

[Potential location of Fig. 5]

211

212

213

214

215

216

217

218

219

220

221

222

223

224

225

226

227

228

229

Kinetic properties of AL-CTPP and CTPP in various water content

The enhancement of emission in AL-CTPP comes from the immobilization of CTPP on lignin polymer. The structure of lignin-based porphyrin polymers is different from that of linear polymers. Lignin backbone structure mainly consists of numerous aromatic units, namely hydroxyphenyl (H), guaiacyl (G), and syringyl (S) units. These similar repeated units are randomly linked by several kinds of bonds, namely β -O-4, β -5 and β - β linkages, to form a complex matrix structure. 50, 51 The complex structure led to strong steric hindrance that limited the motions of porphyrin moieties in the polymers.⁵² It is highly possible that strong steric hindrance of lignin backbones prevents CTPP from aggregation with neighboring porphyrins, which cause emission quenching. To have better understanding and support the role of lignin backbone in our product, we have compared the emission kinetics of CTPP and AL-CTPP. Table 2 listed out the lifetime of the emission peak at 652 nm of CTPP and AL-CTPP in various pH and water fractions. It is interesting to compare the lifetime of AL-CTPP and CTPP monomer in high water fractions to have a glimpse on the role of lignin polymer in AL-CTPP. Examination of the kinetics of the emission peak at 652 nm, in pure ethanol, both CTPP and AL-CTPP were found to have similar emission lifetime are ~ 11 ns. Figure 6 depicted the kinetic of CTPP and AL-TCPP in different water fraction in pH = 7. There is dramatic difference in the kinetic lifetime which suggested that two different species are

present in the solution. Closer examination of the kinetics by two-exponential function; in high water fraction ($f_w \ge 80\%$, pH = 7) environment, there are two species present in both AL-CTPP and CTPP. In the case of CTPP, the two species can be assigned to free monomer species (~5 ns) and self-aggregated species (0.4 ns). Previous ultrafast dynamics study on Porphyrin-Catechol compound reported that aggregation in aqueous solution will form two emissive species, with one in nanosecond time scale and another with sub-nanosecond lifetime. 40 Similar behavior is also found in CTPP monomer case and the results agreed with previous research.⁴³ With decoration of lignin polymer with CTPP, a different set of emissive species is found. One species with ~8 ns lifetime is observed in the emission spectrum. This species is attributed to non-aggregated free CTPP since it has similar lifetime compared with the reference CTPP. Another short lifetime species in AL-CTPP is obtained in the kinetic analysis (~2 ns). This species has much longer lifetime than the self-aggregated species in CTPP. This evidence revealed that the porphyrins in AL-CTPP do not aggregate with neighboring porphyrins and subsequently not causing ACQ. The short lifetime species in AL-CTPP is plausible to be contributed by the π -stacking species between porphyrin and the phenolic moieties on the lignin polymer. The AL-CTPP nanoparticles will be held together more tightly by hydrophobic and π -stacking effects. Since the distance between porphyrin moieties and phenol groups on lignin is reduced, the π - π interaction between them will become important. Therefore, a new complex is formed between porphyrin and the backbone. However, the transition moment and molecular orbitals (MO) energy of lignin units do not match with CTPP, the stacking species do not have efficient coupling and relative weak quenching effect. All in all, our results corroborate the studies proposing about ACQ effect can be greatly reduced by the steric effect and immobilization of porphyrin on polymer.⁵³⁻⁵⁶ It showed the positive correlation between the abilities of ACQ resistance and porphyrin derivatives by bulky groups decoration; as the result, the fluorescence enhancement can be achieved by AL-

257

230

231

232

233

234

235

236

237

238

239

240

241

242

243

244

245

246

247

248

249

250

251

252

253

254

255

256

CTPP.

Heavy metal ions detection of AL-CTPP nanoparticles

Reliable technologies for detection of metal ions in environmental or biological systems are under extensive investigations.⁵⁷ Porphyrins and their derivatives have been proven useful in metal ion detection with high selectivity and sensitivity.^{28, 58} The four-nitrogen-containing macrocycle of porphyrin core is known to stabilize metal ions and hence been widely used in sensor and sorbent.⁵⁹ AL-CTPP demonstrates similar property in heavy metal ions sensing. Five common contaminant metal ions (Mn²⁺, Ni²⁺, Co²⁺, Cu²⁺, Zn²⁺) have been used to test the sensing property of AL-CTPP. This typical sensor protocol relies on the increase in absorbance intensity of the metal ions binding on the porphyrin chromophores in AL-CTPP. Figure 7 showed that AL-CTPP have good correlation between UV-vis absorption changes and the concentration of the metal ions in ppm level. Since different metal porphyrin complexes have different measurement wavelengths and absorption coefficients, this property can help us to differentiate the metal ions in real life water samples.

[Potential location of Fig. 7]

Conclusion

In this work, we demonstrated an innovative new functional product from wastes derived lignin. Alkali lignin was modified by linkage with porphyrin. This linkage brought many mutual benefits to the two functional components in various conditions. Two highlights of the benefits of the new polymer include (a) extension of UV-vis absorbance and photoluminescence regions of lignin; and (b) enhancement of solvent compatibility of porphyrin, especially in the water dominant environments with various pH, AL-CTPP showed the abilities to overcome ACQ and favor photoluminescence performance. In the optical studies the AL-CTPP showed comparable emission characters of porphyrin, such as

large stokes shift and emission wavelength (600-780 nm) under red and NIR fluorescence region. Emission in this region is important for distinguishing the excitation source and the signals and is suitable for biological applications, as they are not obscured by biomolecules, low scattering and long penetration depth. Additionally, linear correlations were found between the absorbance of AL-CTPP and concentrations of several types of heavy metal ions, suggesting the potential to serve as a heavy metal sensor. To conclude, from the point of view of lignin valorization, it is advantageous to decorate lignin nanoparticle by linkage with porphyrin, a multi-functional chemical module to broaden the application to large range of areas and extend the capability of its monomer, like coatings, bio-imaging, sensor of various chemicals, drug delivery and antimicrobial materials. This will impose positive impact in green chemistry and society sustainability.

Experimental Methods

<u>Materials</u>

Alkali lignin (AL), separated from poplar pulping black liquor, was supplied by Shixian Papermaking in Jilin Province, China. The MW of the AL used here was estimated to be 6471 by GPC. Total hydroxyl group is estimated by 31 P NMR which described previously 60 , for the aliphatic groups: 0.35 mmol/g and total hydroxyl groups: 2.92 mmol/g. By elemental analysis, the contents of elemental carbon, hydrogen, and oxygen of AL were measured to be 60.01, 6.03, and 33.06 wt %, respectively. 4-carboxybenzaldehyde, benzaldehyde, triphenylphosphine and Diethyl azodicarboxylate were reagent grade and all metal chloride salts were analytical grade and purchased from J&K Chemistry Co. Ltd and. Deionized water (resistivity of \geq 18 M Ω /cm) was obtained from a Millipore water purification system and used in our experiments. Other reagents are of reagent grade, and solvents were used as received without further purification.

Synthesis of 5-(4-carboxyl phenyl)-10,15,20-triphenyl porphyrin (CTPP)

5-(4-carboxyl phenyl)-10,15,20-triphenyl porphyrin was synthesized by the method modified from pervious described⁶¹. In a 500 mL neck round bottom flask, 1.5 g (10 mmol) of 4-carboxybenzaldehyde and 3.19 mL (30 mmol) of benzaldehyde were dissolved in 200 mL of propanoic acid at 80 °C and the reaction mixture was magnetically stirred. When the solid-aldehyde was fully dissolved, freshly distilled pyrrole (2.8 mL; 10 mmol) was added to the mixture, the temperature then brought to reflux for 2 hrs. The reaction mixture was cooled to room temperature, then was placed in the freezer overnight for porphyrin precipitation. The reaction mixture was then vacuum filtered, and a dark purple solid was obtained, washed by hot deionized water to remove excessive acid and water-soluble impurities. The crude product mixture was purified by column chromatography with solvent using ethyl acetate with 1% THF. The purified product as purple solid was yielded after rotary evaporation.

Preparation of Lignin-based Porphyrin Polymer Complex (AL-CTPP)

0.5g alkali lignin, 0.3g 5-(4-carboxyl phenyl)-10,15,20-triphenyl porphyrin and 0.24g triphenylphosphine were dissolved in 15 mL of a freshly distilled tetrahydrofuran (THF), the reaction mixture was magnetically stirred under room temperature. When the reaction mixture was fully mixed and dissolved in ethyl acetate, the 0.15mL diethyl azodicarboxylate was added as dropwise. Then the reaction was heated to 65 °C for 12 hrs. The final solution was transferred to a dialysis bag (MW = 1000 Da) and dialyzed in THF to remove the triphenylphosphine oxide and unreacted porphyrin. The lignin-based porphyrin polymer solid products were obtained by freeze-drying for 36 hrs.

Characterization

¹H and ¹³C nuclear magnetic resonance (NMR) spectra of the products were determined on a JEOL, ECZ500R, 500MHz NMR spectrometer using DMSO-d₆ as the solvent at 25 °C. The molecular weights and molecular weight distributions were measured by using gel permeation chromatography (GPC). The weight-averaged molecular weight (M_w) and number-averaged molecular weight (M_n) of the lignin samples were measured by GPC as

described previously.⁶² Briefly, lignin samples were dissolved in Dimethylacetamide with addition of 0.11 M LiCl solution, filtered through a 0.45 mm filter and placed in a 2 mL autosampler vial prior to GPC analysis. The molecular weights were estimated by size-exclusion separation performed on the HPLC equipped with Agilent PLgel MIXED-B column. Elemental analysis of C, H, O and N was conducted with an Elementar Vario EL cube. The colloid morphologies were examined by a scanning electron microscopy (SEM, JEOL Model JSM-6490). The hydrodynamic size of nanoparticles was detected by a Nano-ZS Zeta Sizer (Malvern Instruments Ltd., Malvern, U.K.), where the data were collected and analyzed through three consecutive measurements.

Optical properties Study

The electronic absorption measurements were done using Agilent Technologies 8453 UV-Vis absorption spectrophotometer. Emission experiments were carried out using Edinburgh Instruments FLS980 fluorescence spectrometer. The excitation wavelength used for spectral and TCSPC kinetics measurement were 425 nm and 375 nm respectively. CTPP and AL-CTPP were studied in concentration $\sim 30 \mu M$.

Acknowledgements

The authors thank for the financial support from the Hong Kong General Research Fund (15212317), Environment and Conservation Fund (ECF 85/2017), and Sinopec Chemical Commercial Holding Company Limited. The authors also thank the University Research Facility in Chemical and Environmental Analysis (UCEA) for sample analyses.

364 References

- 1. C. Dong, Y. Wang, H. Zhang and S.-Y. Leu, *Bioresource technology*, 2018, **250**, 102-109.
- 2. E. Sjostrom, Wood chemistry: fundamentals and applications, Elsevier, 2013.
- 368 3. R. J. A. Gosselink, E. de Jong, B. Guran and A. Abacherli, *Industrial Crops and Products*, 2004, **20**, 121-129.
- D. Tian, J. G. Hu, J. Bao, R. P. Chandra, J. N. Saddler and C. H. Lu, *Biotechnology for Biofuels*, 2017, 10.
- 372 5. P. Dongre, M. Driscoll, T. Amidon and B. Bujanovic, *Energies*, 2015, **8**, 7897-7914.
- 6. A. H. Faris, A. A. Rahim, M. N. M. Ibrahim, A. M. Alkurdi and I. Shah, *Journal of Applied Polymer Science*, 2016, **133**.
- V. K. Thakur, M. K. Thakur, P. Raghavan and M. R. Kessler, *Acs Sustain Chem Eng*,
 2014, 2, 1072-1092.
- 8. E. Ten, C. Ling, Y. Wang, A. Srivastava, L. A. Dempere and W. Vermerris, *Biomacromolecules*, 2014, **15**, 327-338.
- 9. N. S. Chen, L. A. Dempere and Z. H. Tong, *Acs Sustain Chem Eng*, 2016, 4, 5204-5211.
- 380 10. L. Dai, R. Liu, L. Q. Hu, Z. F. Zou and C. L. Si, *Acs Sustain Chem Eng*, 2017, **5**, 8241-381 8249.
- 382 11. D. Yiamsawas, G. Baier, E. Thines, K. Landfester and F. R. Wurm, *Rsc Adv*, 2014, **4**, 11661-11663.
- 12. Y. Qian, Q. Zhang, X. Q. Qiu and S. P. Zhu, *Green Chem*, 2014, **16**, 4963-4968.
- 13. W. W. Zhao, B. Simmons, S. Singh, A. Ragauskas and G. Cheng, *Green Chem*, 2016, 18, 5693-5700.
- S. Ishihara, J. Labuta, W. Van Rossom, D. Ishikawa, K. Minami, J. P. Hill and K. Ariga,
 Phys Chem Chem Phys, 2014, 16, 9713-9746.
- 15. S. Singh, A. Aggarwal, N. V. S. D. K. Bhupathiraju, G. Arianna, K. Tiwari and C. M. Drain, *Chemical Reviews*, 2015, **115**, 10261-10306.
- 391 16. X. Dong, C. Wei, L. Lu, T. J. Liu and F. Lv, *Materials Science & Engineering C-Materials for Biological Applications*, 2016, **61**, 214-219.
- 17. L. Z. Zhang, Y. Lin, Y. J. Zhang, R. Chen, Z. S. Zhu, W. Wu and X. Q. Jiang,
 394 *Macromolecular Bioscience*, 2012, 12, 83-92.
- 18. J. F. Lovell, A. Roxin, K. K. Ng, Q. C. Qi, J. D. McMullen, R. S. DaCosta and G. Zheng,
 Biomacromolecules, 2011, 12, 3115-3118.
- P. Couleaud, V. Morosini, C. Frochot, S. Richeter, L. Raehm and J. O. Durand,
 Nanoscale, 2010, 2, 1083-1095.
- 399 20. D. M. E. Freeman, A. Minotto, W. Duffy, K. J. Fallon, I. McCulloch, F. Cacialli and H. Bronstein, *Polym Chem-Uk*, 2016, **7**, 722-730.
- 401 21. C. A. Hunter and J. K. M. Sanders, *J Am Chem Soc*, 1990, **112**, 5525-5534.
- 402 22. Y. J. Wang, Z. Y. Li, J. Q. Tong, X. Y. Shen, A. J. Qin, J. Z. Sun and B. Z. Tang, *J Mater Chem C*, 2015, **3**, 3559-3568.

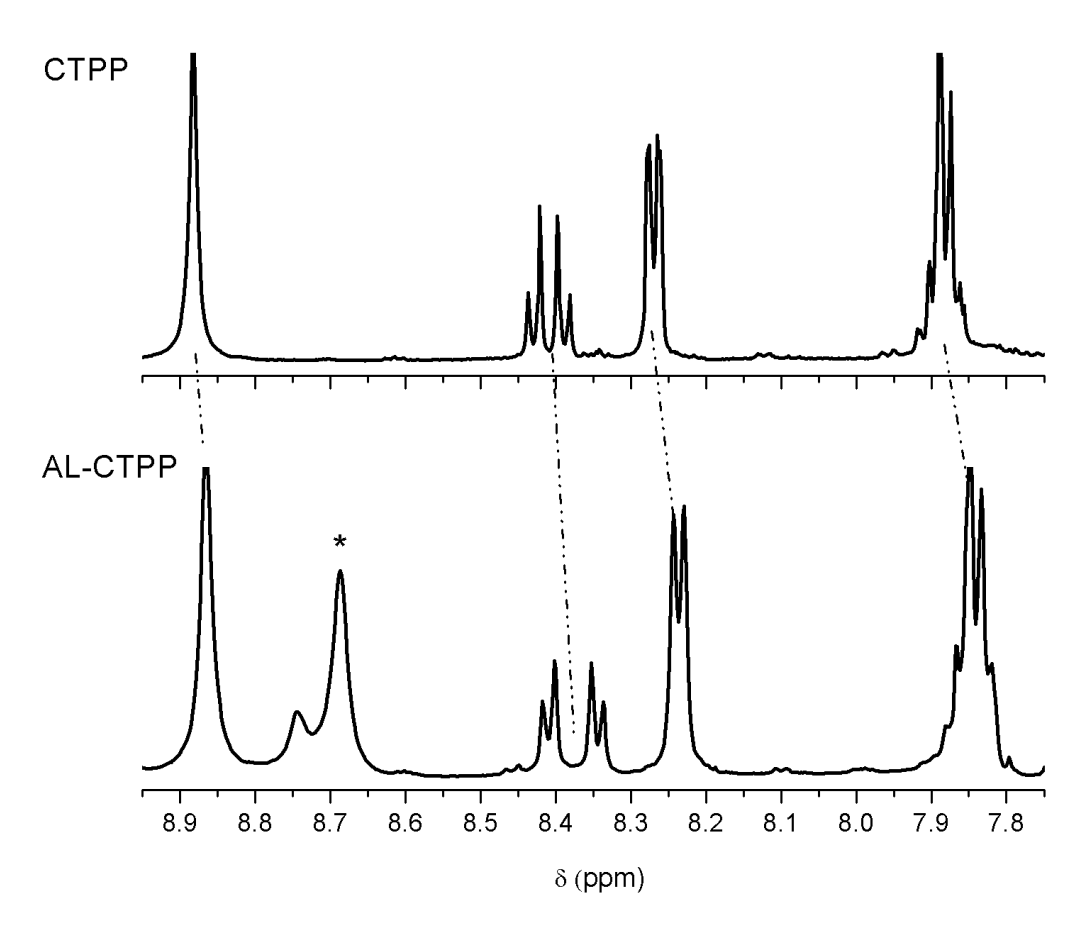
- 404 23. M. Jr, J. M. Perez, C. Bruckner and R. Weissleder, *Nano Letters*, 2005, **5**, 2552-2556.
- 24. A. V. Kondrashina, R. I. Dmitriev, S. M. Borisov, I. Klimant, I. O'Brien, Y. M. Nolan, A.
 V. Zhdanov and D. B. Papkovsky, *Advanced Functional Materials*, 2012, 22, 4931-4939.
- 407 25. C. F. Wu, B. Bull, K. Christensen and J. McNeill, *Angewandte Chemie-International Edition*, 2009, **48**, 2741-2745.
- 26. S. Y. Li, K. W. Chang, K. Sun, Y. Tang, N. Cui, Y. Wang, W. P. Qin, H. Xu and C. F.
 Wu, Acs Appl Mater Inter, 2016, 8, 3624-3634.
- 27. H. N. Kim, Z. Q. Guo, W. H. Zhu, J. Yoon and H. Tian, *Chemical Society Reviews*, 2011,
 40, 79-93.
- 413 28. Z. Fang, K. Y. Pu and B. Liu, *Macromolecules*, 2008, **41**, 8380-8387.
- 414 29. C. Mauriello-Jimenez, J. Croissant, M. Maynadier, X. Cattoen, M. W. C. Man, J.
- Vergnaud, V. Chaleix, V. Sol, M. Garcia, M. Gary-Bobo, L. Raehm and J. O. Durand, J.
- 416 *Mater Chem B*, 2015, **3**, 3681-3684.
- 417 30. K. D. Lu, C. B. He and W. B. Lin, *J Am Chem Soc*, 2015, **137**, 7600-7603.
- 418 31. C. Aggelidou, T. A. Theodossiou and K. Yannakopoulou, *Photochemistry and Photobiology*, 2013, **89**, 1011-1019.
- 32. M. Wu, Z. W. Yu, Y. Liu, D. F. Feng, J. J. Yang, X. B. Yin, T. Zhang, D. Y. Chen, T. J.
 Liu and X. Z. Feng, *Chembiochem*, 2013, 14, 979-986.
- 33. J. S. Sun, Y. L. Chen, L. Y. Zhao, Y. T. Chen, D. D. Qi, K. M. Choi, D. S. Shin and J. Z.
 Jiang, *Chem-Eur J*, 2013, 19, 12613-12618.
- 424 34. S. Fletcher, *Org Chem Front*, 2015, **2**, 739-752.
- 425 35. N. Iranpoor, H. Firouzabadi and D. Khalili, *Org Biomol Chem*, 2010, **8**, 4436-4443.
- 426 36. Y. H. Deng, Y. F. Liu, Y. Qian, W. J. Zhang and X. Q. Qiu, *Acs Sustain Chem Eng*, 427 2015, **3**, 1111-1116.
- 428 37. J. L. Wang, B. Wu, S. Li, G. Sinawang, X. G. Wang and Y. N. He, *Acs Sustain Chem Eng*, 2016, **4**, 4036-4042.
- 430 38. B. Guo, X. L. Cai, S. D. Xu, S. M. A. Fateminia, J. Liu, J. Liang, G. X. Feng, W. B. Wu and B. Liu, *J Mater Chem B*, 2016, **4**, 4690-4695.
- 432 39. T. Ogawa, E. Tokunaga and T. Kobayashi, *Chem Phys Lett*, 2005, **410**, 18-23.
- 433 40. S. Verma, A. Ghosh, A. Das and H. N. Ghosh, *J Phys Chem B*, 2010, **114**, 8327-8334.
- 434 41. S. Mandal, S. Bhattacharyya, V. Borovkov and A. Patra, *J Phys Chem C*, 2012, **116**, 11401-11407.
- 436 42. S. Verma, A. Ghosh, A. Das and H. N. Ghosh, *Chem-Eur J*, 2011, **17**, 3458-3464.
- 43. K. Hosomizu, M. Oodoi, T. Umeyama, Y. Matano, K. Yoshida, S. Isoda, M. Isosomppi,
- N. V. Tkachenko, H. Lemmetyinen and H. Imahori, *J Phys Chem B*, 2008, **112**, 16517-16524.
- 44. U. Rosch, S. Yao, R. Wortmann and F. Wurthner, *Angew Chem Int Ed Engl*, 2006, **45**, 7026-7030.
- 442 45. Y. Deng, W. Yuan, Z. Jia and G. Liu, *J Phys Chem B*, 2014, **118**, 14536-14545.

- 443 46. T. Yamamura, S. Suzuki, T. Taguchi, A. Onoda, T. Kamachi and I. Okura, *J Am Chem Soc*, 2009, **131**, 11719-11726.
- 445 47. R. Rai, V. Kumar and S. Pandey, *Phys Chem Chem Phys*, 2014, **16**, 7263-7273.
- 48. R. F. Pasternack and P. J. Collings, *Science*, 1995, **269**, 935-939.
- 49. M. Zannotti, R. Giovannetti, B. Minofar, D. Reha, L. Plackova, C. A. D'Amato, E. Rommozzi, H. V. Dudko, N. Kari and M. Minicucci, *Spectrochim Acta A*, 2018, **193**,
- 449 235-248.

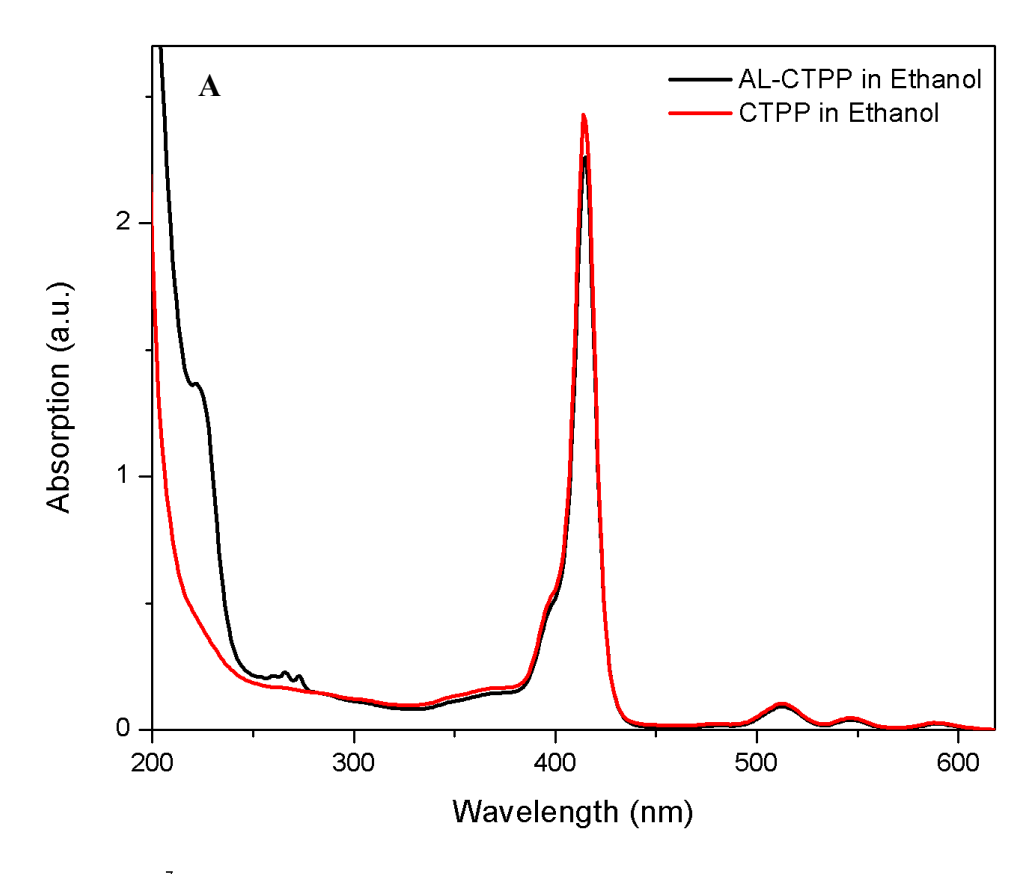
- 50. J. Zakzeski, P. C. A. Bruijnincx, A. L. Jongerius and B. M. Weckhuysen, *Chemical Reviews*, 2010, **110**, 3552-3599.
- 452 51. J. C. del Rio, J. Rencoret, P. Prinsen, A. T. Martinez, J. Ralph and A. Gutierrez, *Journal of Agricultural and Food Chemistry*, 2012, **60**, 5922-5935.
- 52. H. H. Nimz, U. Tschirner, M. Stahle, R. Lehmann and M. Schlosser, *Journal of Wood Chemistry and Technology*, 1984, **4**, 265-284.
- 456 53. S. Liu, C. Hu, Y. Wei, M. Duan, X. Chen and Y. Hu, *Polymers-Basel*, 2018, **10**.
- 457 54. T. Higashino and H. Imahori, *Dalton T*, 2015, **44**, 448-463.
- 458 55. A. D'Urso, M. E. Fragala and R. Purrello, *Chem Commun (Camb)*, 2012, **48**, 8165-8176.
- 459 56. K. Ladomenou, T. N. Kitsopoulos, G. D. Sharma and A. G. Coutsolelos, *Rsc Adv*, 2014,
 460 4, 21379-21404.
- 57. Y. T. Shen, G. Mackey, N. Rupcich, D. Gloster, W. Chiuman, Y. F. Li and J. D. Brennan,
 Anal Chem, 2007, 79, 3494-3503.
- 58. M. Anju, T. Divya, M. P. Nikhila, T. V. A. Kusumam, A. K. Akhila, V. A. Ansi and N. K. Renuka, *Rsc Adv*, 2016, 6, 109506-109513.
- J. Yang, Z. Wang, K. L. Hu, Y. S. Li, J. F. Feng, J. L. Shi and J. L. Gu, *Acs Appl Mater Inter*, 2015, 7, 11956-11964.
- 467 60. J. S. Lupoi, S. Singh, R. Parthasarathi, B. A. Simmons and R. J. Henry, *Renew Sust Energ Rev*, 2015, 49, 871-906.
- 469 61. A. D. Adler, F. R. Longo, F. Kampas and J. Kim, *J Inorg Nucl Chem*, 1970, **32**, 2443-&.
- 470 62. O. Ringena, A. Lebioda, R. Lehnen and B. Saake, *J Chromatogr A*, 2006, **1102**, 154-163.

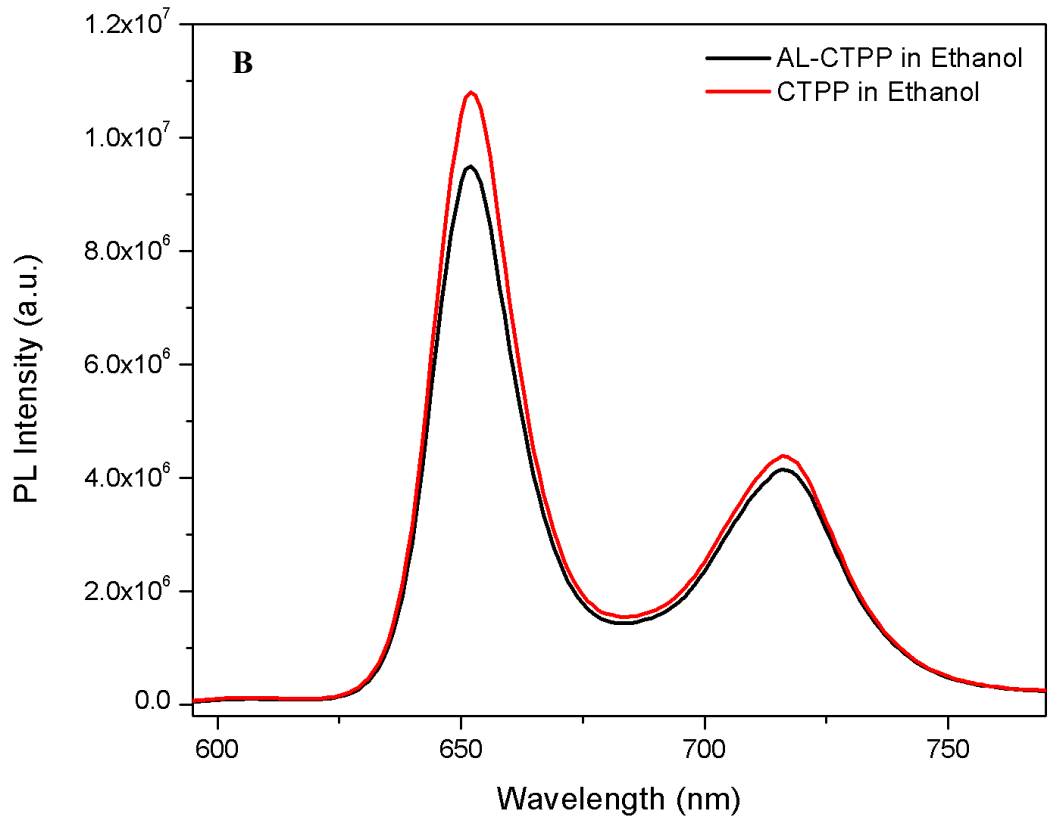
473	Figure captions
474	Fig. 1 Proposed structure formula of AL-CTPP
475	Fig. 2 ¹ H NMR spectra of CTPP and AL-CTPP
476	Fig. 3 (A) UV-vis absorption and (B) photoluminescence spectra (excitation at 425 nm) of
477	CTPP and AL-CTPP (30 µM in ethanol)
478	Fig. 4 Effect of various pH on AL-CTPP Nano-particles size and the inset shows the SEM
479	images of (A) CTPP & (B) AL-CTPP.
480	Fig. 5 (A) UV-vis absorption of CTPP and (B) AL-CTPP from $f_w = 0.20$ -0.95 (C) PL
481	(excitation at 425 nm) intensity of CTPP and AL-CTPP pH 3-7, $f_{\rm w}$ = 0.95 (D) PL intensity
482	(excitation at 425 nm) of CTPP and AL-CTPP from $f_w = 0.70$ -0.95
483	Fig. 6 Normalized emission dynamic of CTPP and AL-CTPP at 652 nm in $f_w = 0.60$ and 0.80
484	Fig. 7 UV-vis absorption titration of AL-CTPP with various concentrations of Ni ²⁺ , Co ²⁺ ,
485	Mn ²⁺ , Zn ²⁺ , Cu ²⁺ metal ions. Intercepts have been normalized for comparison. Original figure
486	can be found in supporting information
487	
488	

491 Fig. 1

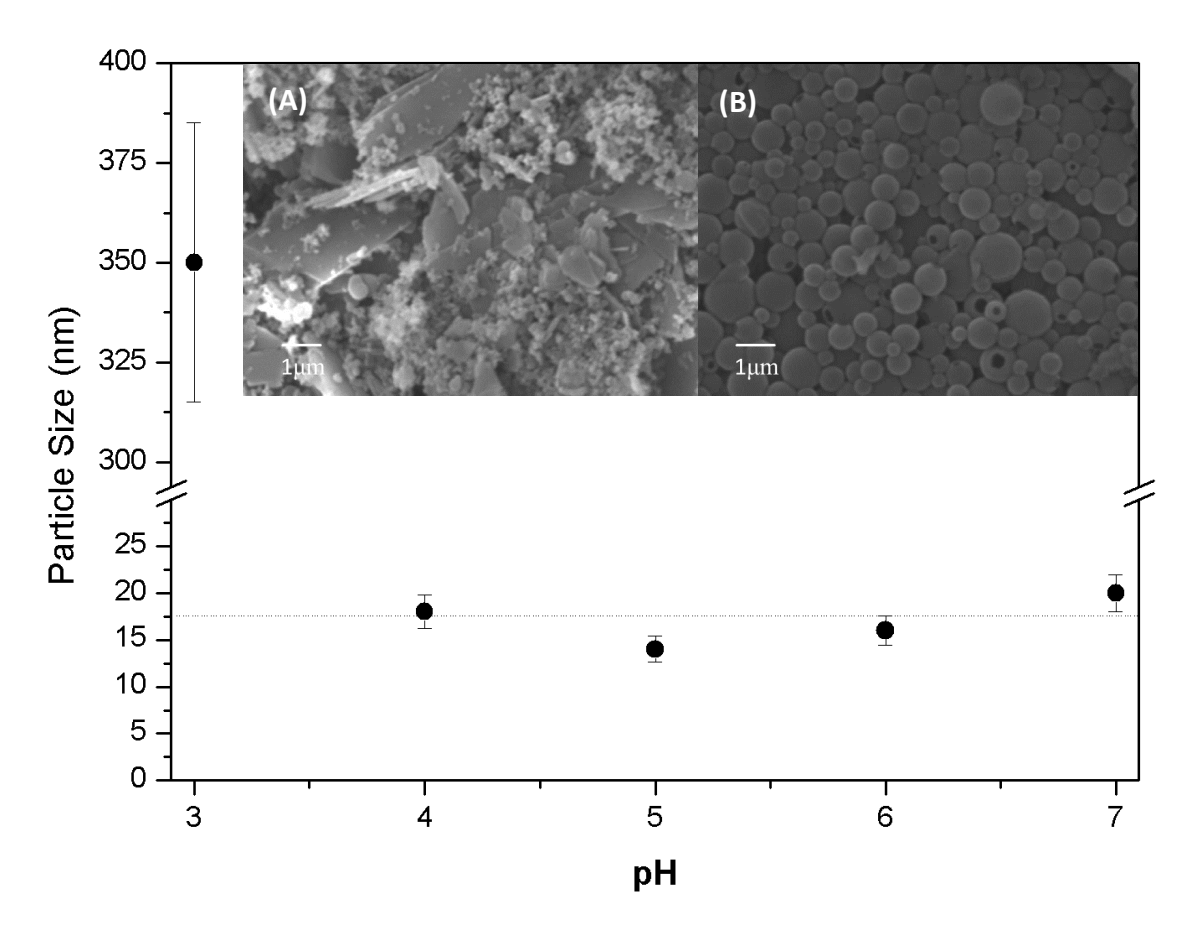


495 Fig. 2

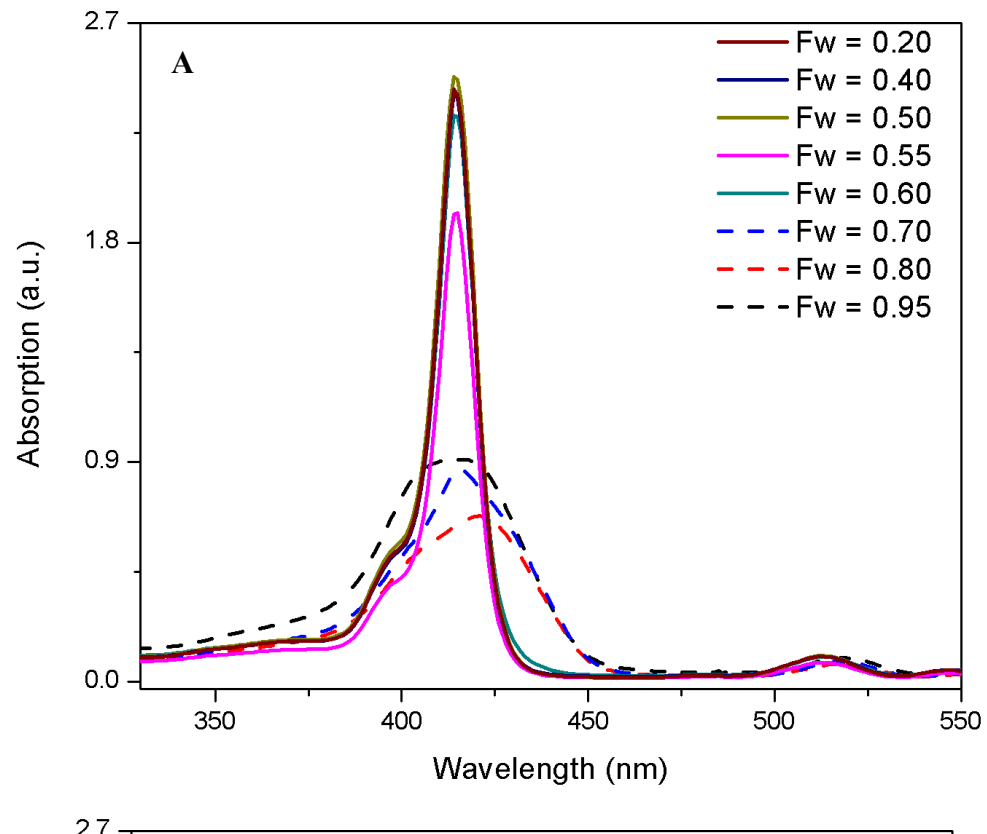


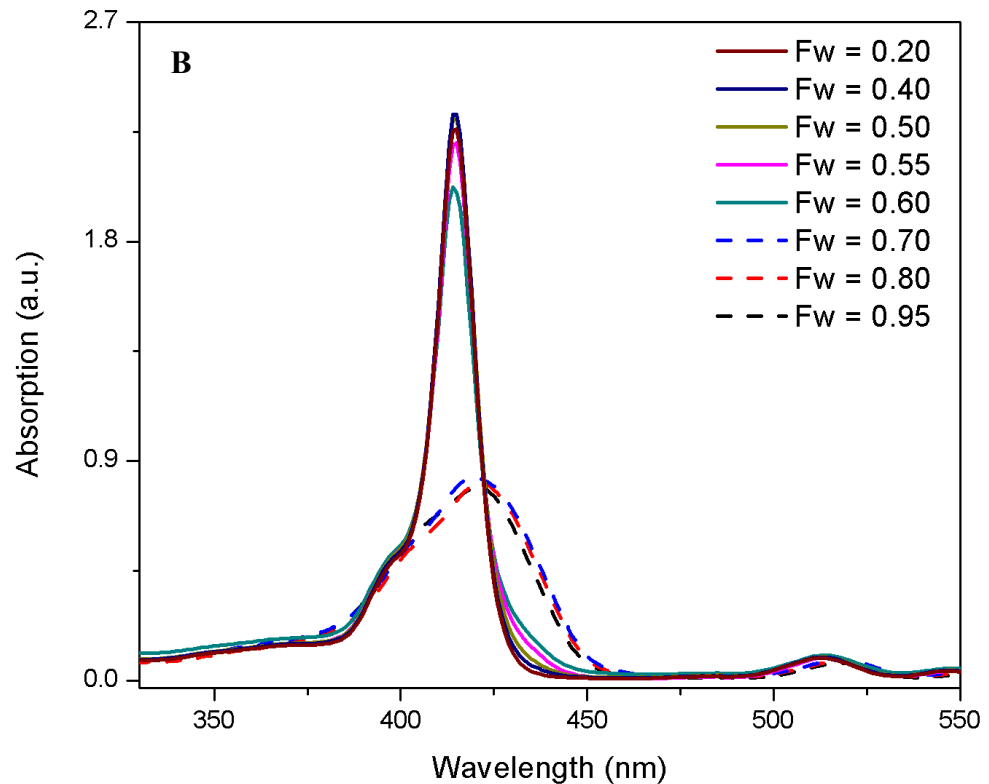


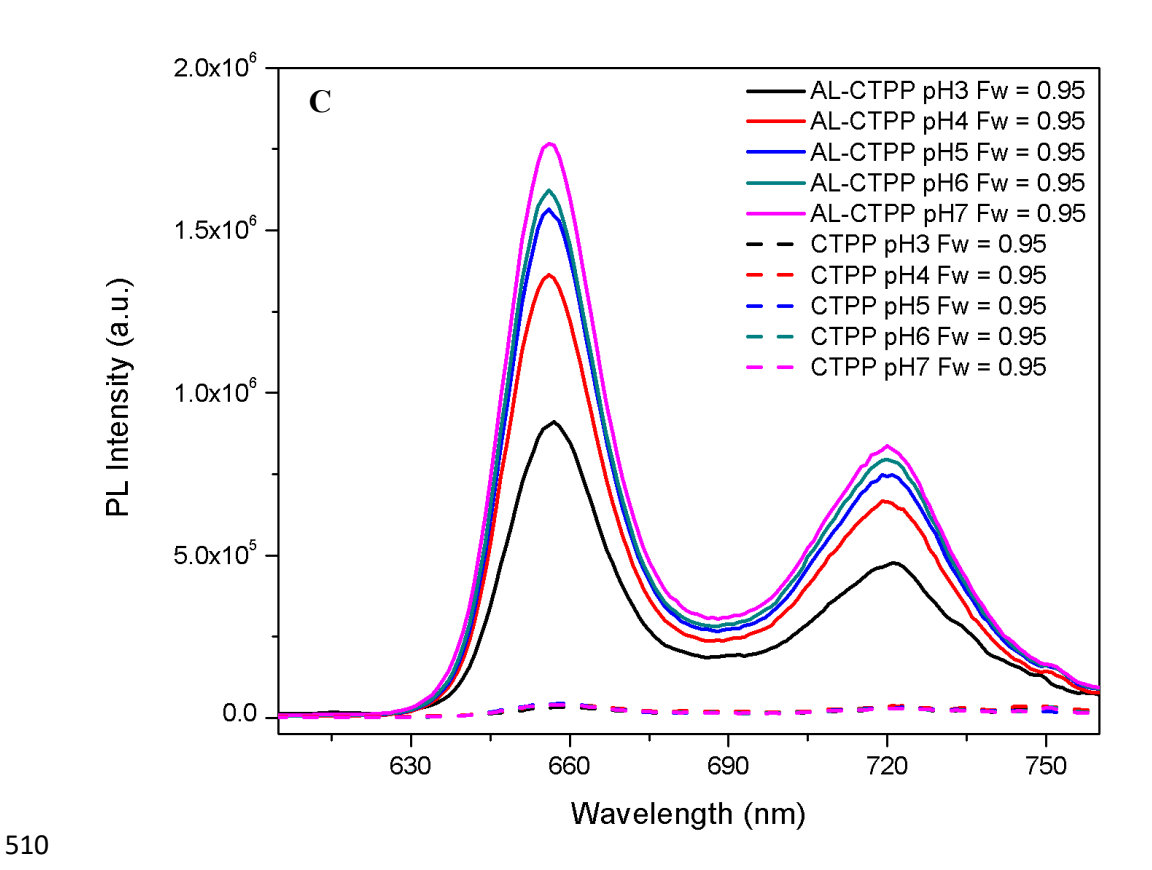
500 Fig. 3

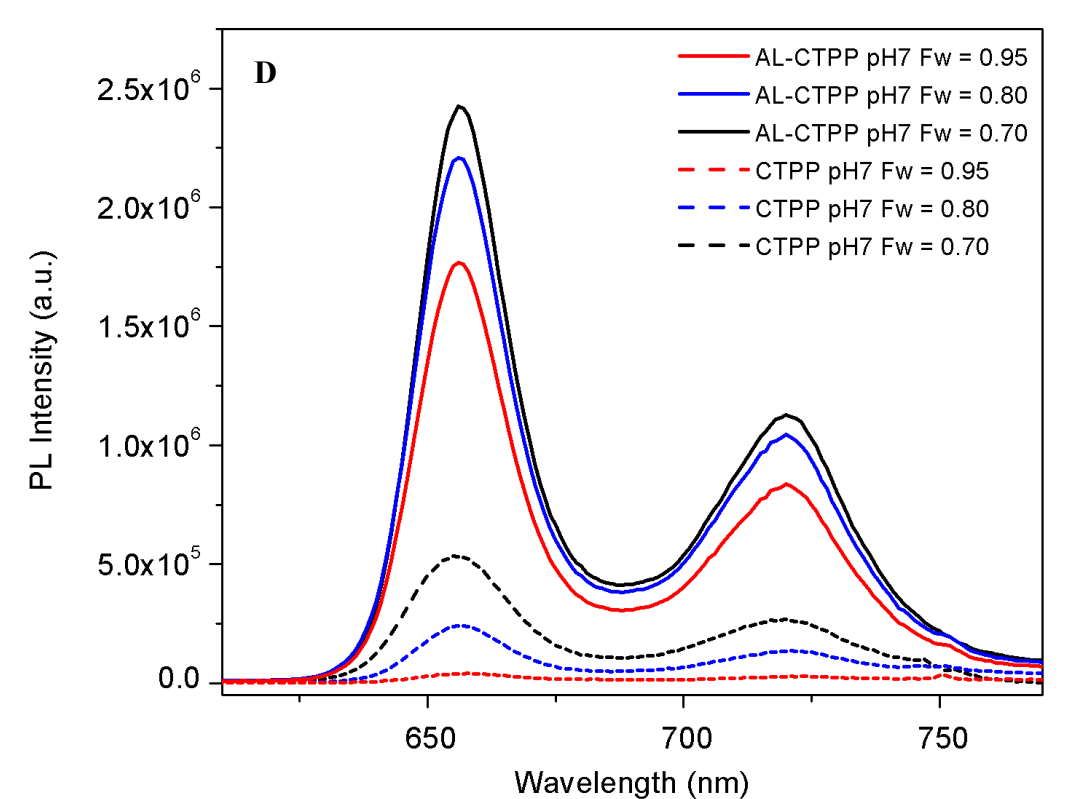


506 Fig. 4

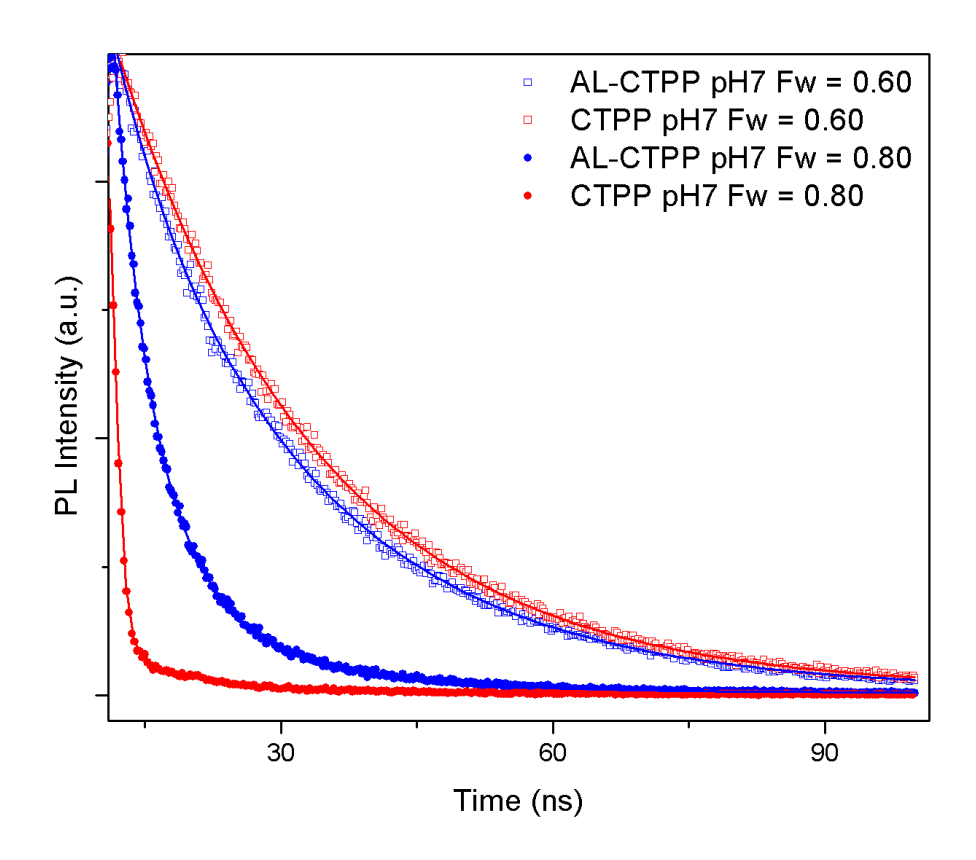








514 Fig. 5



517 Fig. 6

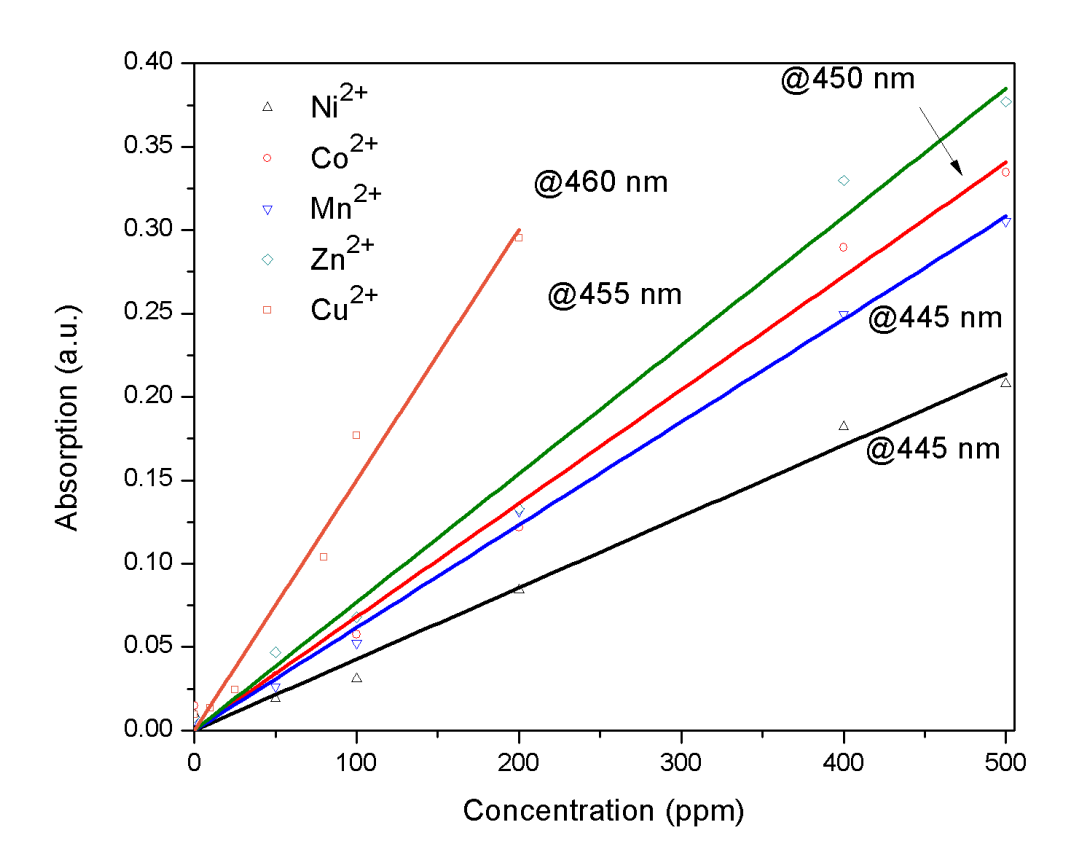


Fig. 7

Table 1. Elemental analysis and degree of functionalization of AL-CTPP (unit: %)

Sample	N	С	Н	О	DF
AL	0.00	60.01	33.06	6.03	-
AL-CTPP	0.67	60.23	33.27	5.91	41.23

Table 2. Emission lifetimes (nanosecond) of CTPP and AL-CTPP in different solvent conditions after excitation 375 nm and monitoring at 652 nm

	СТРР	AL-CTPP	СТРР	AL-CTPP	СТРР	AL-CTPP	СТРР	AL-CTPP
Fw	0.95		0.80		0.55		0.20	
рН3	NI/D	2.14	3.67	6.32	11.37	11.31	10.41	10.39
	N/D	0.82	0.24	1.25	0.63	1.80		
411 4	N/D	2.19	3.94	6.79	11.26	11.15	10.50	10.46
pH4		1.01	0.31	1.95		2.55		
115	N/D	2.68	4.78	6.72	11.32	11.24	10.50	10.47
pH5		1.15	0.33	1.97		2.66		
ъЦ6	N/D	3.18	5.49	7.14	11.30	12.06	10.53	10.59
pH6		1.26	0.39	2.06		5.36		
II7	N/D	3.54	5.49	7.81	11.39	12.17	10.57	10.61
pn/		1.35	0.40	2.17		6.32		